Journal of Energy Storage 114 (2025) 115833

Contents lists available at ScienceDirect

Journal of Energy Storage

journal homepage: www.elsevier.com/locate/est

Research papers

State of charge (SOC) estimation in electric vehicle (EV) battery management systems using ensemble methods and neural networks

Edward Ositadinma Ofoegbu *

School of Built Environment, Engineering and Computing, Leeds Beckett University, Leeds, United Kingdom

ARTICLE INFO

Keywords:
State of charge
Lithium-ion battery
Feed forward neural networks
Electric vehicles
Battery management system
Machine learning

ABSTRACT

Battery management systems (BMS) are critical in ensuring the performance, reliability, and safety of battery systems through accurate estimation of the State of Charge (SOC) of batteries. As on-board SOC estimation, together with other functionalities by the BMS can result in its high design complexity, high cost, and high energy consumption, this study explores a data-driven estimation of a Lithium battery state of charge (SOC) while discharging, using simple linear regression, ensemble methods, and neural networks respectively to ensure an accurate low time complexity solution as compared to existing methods. A known dataset of 835,248 records from Li [NiMnCo]O2 (H-NMC)/Graphite + SiO battery was used to train and test each model to determine the best fit. This study determined that neural networks are the models of choice for SOC prediction instead of linear and ensemble regression. Still, also the wide tri-layered feed-forward neural network proposed in this study showed great results by having a maximum error percentage of less than 1 %, and a mean squared error (MSE) of 1e-08, which is similar to or better than what is obtainable in other more complex deep neural network variants such as the Gated recurrent unit recurrent neural network (GRU-RNN), with an MSE of 1e-06 and similar load classifying neural network models with an error percentage of 3.8 %. The FFNN proposed in this study also has the advantage of having lower technical and time complexity computational costs required for active fault estimation in thin client devices such as a BMS.

1. Introduction

Battery management systems, simply regarded as BMS in literature as well as in practice are critical systems deployed in electric vehicles and other related battery-powered systems. The major function of the BMS is to evaluate the state of charge (SOC), predict system health, thermal control, charge equalization, protection, optimal power consumption, and energy utilization [1]. The State of charge (SOC) is a critical output estimated by the BMS, as it signifies a direct relationship between the overall battery capacity and the remaining battery capacity under different load and charge/discharge conditions. A mathematical representation of the SOC of a battery, estimated using the battery current, battery voltage, and battery temperature is defined as

$$SOC = \frac{Q_{Remaining}}{Q_{Rated}} \tag{1}$$

where the remaining charge in the battery is depicted $Q_{Remaining}$, while Q_{Rated} depicts the battery-rated-capacity when a battery is put under different load conditions and various charge/discharge cycles, Q_{Rated} never remains the same throughout the lifetime of the battery as non-uniformities during the manufacturing process of the battery, as well as external conditions not limited to aging, ambient temperature, and state of health all contribute to the variability in Q_{Rated}.

Climatic concerns as well as the energy crisis prevalent in many climes, have increased the demand for clean energy provisions. Green agriculture, green infrastructure, sustainable transport, and other net zero carbon and sustainability initiatives are poised to sustain an energy utilization paradigm shift in the next few decades. Electric vehicles and their hybrid counterparts have the potential to play a key role in this shift as systems driven by energy storage systems (ESS) offer fewer possibilities for environmental degradation as opposed to fossil-based options.

Energy storage systems (ESS) have evolved, with active research currently underway to develop far better solutions with attractive features such as a long lifespan of energy source, low battery self-discharge, high energy density, high voltage, and a lot more features. The Lithium-ion battery currently offers the best performance related to the desired

* Corresponding author.
E-mail address: e.ofoegbu@leedsbeckett.ac.uk.

https://doi.org/10.1016/j.est.2025.115833
Received 18 September 2024; Received in revised form 8 January 2025; Accepted 11 February 2025
Available online 20 February 2025

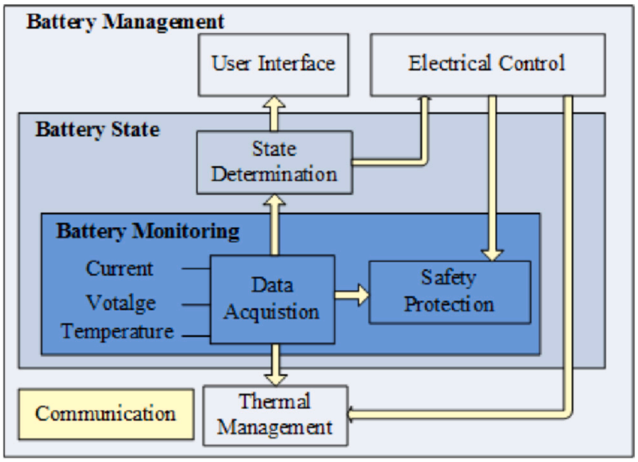

Fig. 1. Illustration of a battery management system [3].

characteristics expected for an energy storage system (ESS) [2]. Many devices beyond electric vehicles utilize Lithium-ion batteries as their main power source and thus managing the operational and specification characteristics of Lithium-ion batteries to ensure optimal performance and safety is a key service that battery management systems provide.

Battery management systems (BMS) in Electric vehicles, as depicted in Fig. 1, are the primary means of managing the power components that drive electric vehicles. They are well-designed circuits that monitor the charge/discharge current, voltage, and temperature of each cell in the battery pack.

This study investigates the application of ensemble methods and artificial neural networks for predicting the state of charge (SOC) of the Lithium-ion battery, by the battery management system deployed in electric vehicles. Fault tolerance within the system can be achieved, if possible, where faults that could cause fires are detected earlier based on the predictive estimation of the state of charge of the deployed battery system. MATLAB and its associated applications are used for the training, testing, and validation of the results of this study.

2. Literature review

State-of-charge (SOC) estimation has long been a subject of intensive research driven by the difficulties in its accurate estimation. Estimating the state of charge traditionally encounters problems such as long-term state divergence, offset, and drift [4]. The authors in [4] introduced a nonlinear predictor based on the extended Kalman filter for estimating the state of charge in a lead-acid battery utilized in hybrid electric vehicles. The proposed technique was chosen as it offered promise to overcome the challenges of state divergence, offset, and drift, and by determining the SOC based on the voltage present in a bulk capacitor when the value of the surface capacitor is kept constant, the study was able to achieve an estimation accuracy of 3 %. Variations of the Kalman filter were also used as was observed in [5], for which an unscented Kalman filter was used to reduce the errors due to a neural network-based SOC estimation model. The neural network was used to model the SOC as a function of system measurements, with an attempt to eliminate the open circuit voltage and state of charge relationship (OCV/SOC) benchmarked in most studies to date. These sampled studies above represent the various estimation methods currently used in recent studies for estimating the state of charge of a Lithium-ion battery. The SOC of batteries used in electric vehicle design, specifically the lithium-ion battery is an integral energy storage component utilized by the BMS for moderating the internal state of the overall system. SOC estimation has always been done at the same time or in the same context as a state of health (SOH) estimation, which is moderated by the resistance (R measured in Ω) and capacity (E measured in Ah) of a battery. However wrong or inaccurate estimation of state of charge (SOC) has been linked to performance decay, accelerated aging, and hazardous incidents in Lithium-ion batteries used in electric vehicles [6].

There are therefore different methods for estimating the SOC of a battery. The modeless approach which predominantly features the Coulomb counting method [7] and model-based observers [8] actively utilizes different versions of the Kalman filter, while the data-driven non-linear method [6] consists mainly of neural network-based predictive models. The neural networks are used on experimental data on battery systems, generated in various charge/discharge conditions. The applicability of neural networks as a possible technique for the estimation of SOC, based on the known dynamic behaviors of Li-ion battery types was explored in [9], Related neural network or deep network prediction studies such as in [6] utilized a load-classifying neural network on three pre-categorized battery operation modes, namely idle, charge, and discharge modes. The Parallelized neural network developed in the study was able to give an average estimation error of 3.8 % which according to the authors, compares sufficiently with the results of the model and modeless approaches earlier discussed.

Data-driven models are deemed a good option for estimating SOC as they are simple to implement and yet powerful due to their dependence not only on the quality of training data available but also on the small computation cost of its implementation. The aging of battery systems plays a key role in the SOC of the battery as well as in the ability to accurately estimate the SOC as demonstrated in [10], who utilized a radial basis function neural network model based on the life cycle model of a 6 Ah Lithium-ion battery to show that there exists a direct relationship between the rate of battery aging and the accuracy of the SOC estimate obtained. The study also implied that the accuracy would differ based on different temperatures and loading profiles.

SOC has a relationship with the open circuit voltage (OCV) of a lithium battery and neural networks can express this relationship as was discussed in [11], where an artificial neural network (ANN) was trained with current and voltage as direct input to the neural network, while the SOC was the output of the network. The study further highlighted the fact that single-layered neural networks can capture the non-linear characteristics of a battery. The impact of temperature on the accurate estimation of SOC was also expressed by [12] who utilized a time delay neural network algorithm optimized with an improved firefly algorithm to estimate the SOC of the Lithium Nickel Cobalt Manganese ($LiNiMnCoO_2$) battery in different temperatures and Electric vehicle drive cycles. The study determined that optimized neural networks performed better in SOC estimation than un-optimized variants, with the study obtaining a root mean square error (RSME) below 1 %. Similar studies have obtained error rates that validate the accuracy of the neural network as an appropriate technique for the estimation of SOC, as [13] utilized a non-linear autoregressive with external input (NARX) neural network to estimate the SOC of battery systems in Electric vehicles under different drive conditions. The Mean square error of estimates was observed in the study to lie less than 1e-6, for all the tested drive cycles. The mean square error and the root mean square error have been used as a measure to determine the accuracy of the different models tested in diverse studies to date for the estimation of SOC through data-driven methods. To achieve high accuracy of prediction, optimization methods have also been considered in numerous studies such as the use of the recurrent neural network with gated recurrent units for accurate estimation of the SOC of batteries with sophisticated dynamics and changing ambient conditions [14]. Where the results of the study based the choice of the algorithm on the proliferation of easy access to high computing facilities, specifically graphical processing units. An RMSE of 3.5 % was obtained for untrained temperature considerations in this study, which further demonstrated the capacity of neural networks to estimate the SOC of a battery. A few studies have combined the different estimation methods, such as [15], which used an artificial neural network (ANN) to estimate the SOC of a LiFePO4 battery based on its current and voltage readings, and the resultant open circuit voltage (OCV) relationship,

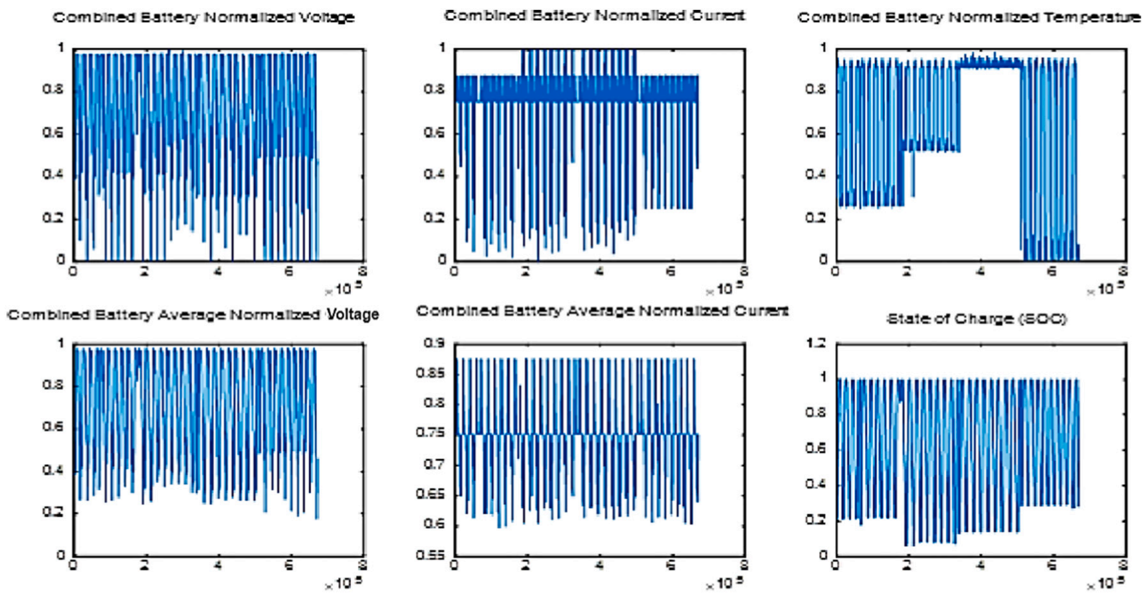

Fig. 2. Training dataset profile describing the features of (a) voltage, (b) current, (c) temperature, (d) average voltage, (e) average current, and (f) state of charge.

while a scented Kalman filter was utilized to reduce the errors in the estimated SOC values. Deep neural networks (DNN), gated recurrent unit recurrent neural networks (GRU-RNN) and an artificial neural network (ANN) were used in [16] to compare the SOC values obtained from simulation and those obtained from experimentation, where results in different load conditions showed a minimum error rate of 0.5 %, which in comparison with a Deep neural network proved its efficiency as an estimator of the SOC of a lithium-ion battery. Other neural network variants and techniques such as Deep neural networks [17], autoencoders, and long short-term memory neural networks [18], feedforward neural network (FFNN) used together with an extended Kalman filter (EKF) [19], deep feed-forward neural network (DFFNN) with LSTM [20] are all different techniques that have been applied for the estimation of SOC with differing results. This study is aimed at first comparing the neural network performance with standard ensemble regression methods to validate its performance as a better option in SOC estimation and to validate the potential of neural networks and their optimized variants as the technique of choice for data-driven estimation of the state of charge of Lithium-ion batteries.

Some of the gaps in literature can be seen from the work in [17], where the authors suggest that the optimal number of layers for a deep neural network should lie between three and four layers, where the tri-layered network in their view performed best in training, but the four-layer DNN performed best in testing in different drive cycles, thus they were of the view that higher number of layers or epoch values did not necessarily improve the model performance but rather increased the error rate, the optimal number of nodes required or the layers was also a research focus in [6], who in their opinion determined that the number of nodes in each layer did not have any beneficial effect on the performance of the model, but also observed that the number of layers played a role in how accurate the results of the neural network would be, the study also settled on the possibility that a Tri-layered network performed best with an average SOC estimation error of 3.8 %. However other studies presented results with models using a higher number of layers.

State of charge (SOC) can be estimated in isolated and combined operational modes, thus a model's performance is dependent on the battery operational mode being considered in each study. While this study focuses on the state of charge estimation in discharge mode, it must be mentioned that the introduction of additional variables such as driving conditions, combined idle/charge/discharge mode, and consideration of extreme operational temperatures affect the performance and overall accuracy of the model. Advanced methods such as improved singular filtering-Gaussian process regression-long short-term memory model [21], which achieved excellent whole life cycle capacity estimation considering fast charging and multi-current variations is an example of the above. The result of the study was based on the equally excellent results obtained in [22] which established the strengths of anti-noise adaptive long short-term (LSTM) models in useful life prediction for Lithium batteries. LSTM as a method is proving itself a great candidate for state-of-charge estimation in combined mode as verified by the results of very recent studies in [23], who proposed a novel random search-optimized LSTM model, that combined the search strengths of the random forest algorithm to improve the accuracy of the LSTM model.

Optimized variants of the LSTM models are also being seen with innovations proposed in [24], which used particle swarm optimization on an LSTM network to good effect once again highlighting the future possibilities LSTM offers for combined mode estimation with varying operational considerations in battery systems. The main contributions of this work are highlighted below

- An accurate comparison of non-neural network models and neural network models was made on experimentally measured data relating to the Li [NiMnCo]O2 (H-NMC)/Graphite + SiO battery in fast and normal charge current conditions.
- The proposed non-neural and neural network models for SOC estimation were trained using the large experimental data, and the models were compared using metrics such as RMSE, MSE, MAE, and R^2.
- Comparison between the non-neural and neural network models demonstrated the superiority of neural network models (wide-FFNN) as an ideal candidate for data-driven SOC estimation in a battery's discharge state.
- A comparison of the FFNN model obtained here and the results of comparative studies such as various variants of LSTM, RNN, and Kalman filter-based estimators, gated recurrent unit recurrent neural network (GRU-RNN), etc. were also compared. A key highlight was

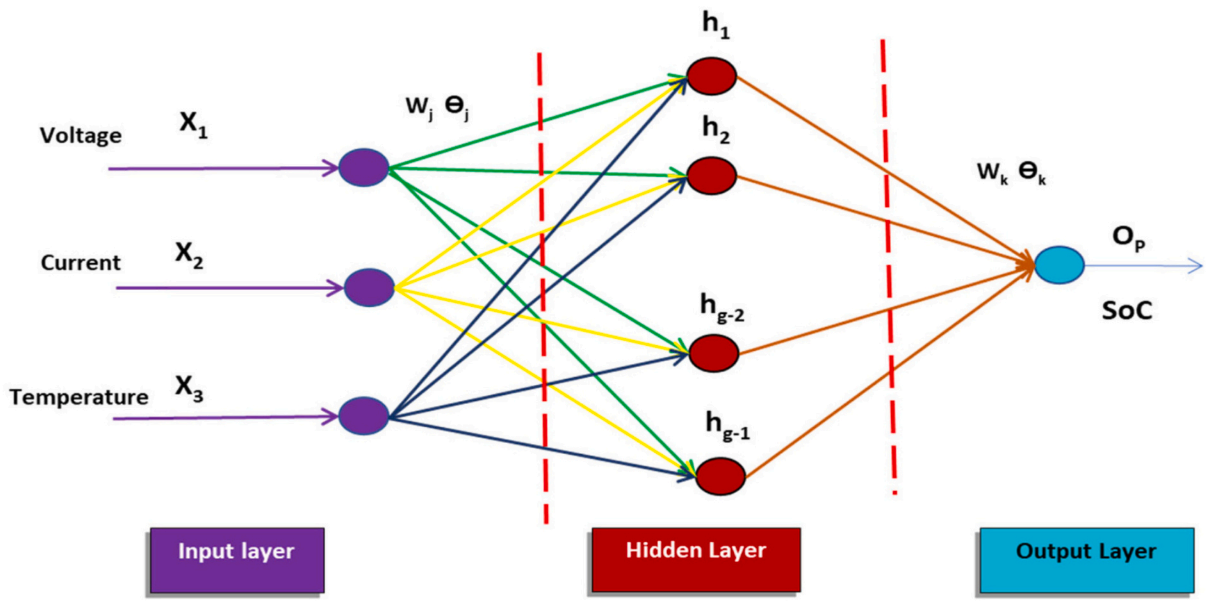

Fig. 3. Conventional feed forward neural network structure [29].

Table 1
Model performance under training and test conditions.

Model	MAE	MSE	RMSE	R-squared
Training				
Linear regression	0.032948	0.0019538	0.044202	0.98
Tree	0.0044787	0.00010445	0.01022	1.00
Ensemble (bagged) tree	0.0040595	0.0000734553	0.0085705	1.00
Ensemble (boosted) tree	0.036311	0.0017021	0.041256	0.98
Testing				
Linear regression	0.034487	0.0020742	0.045543	0.97
Tree	0.015548	0.00064398	0.025377	0.99
Ensemble (bagged) tree	0.014091	0.00052991	0.02302	0.99
Ensemble (boosted) tree	0.036976	0.0019484	0.044141	0.97

in the GRU-RNN study, where results showed that the proposed wide-FFNN network in this study performed better with a mean squared error (MSE) of 1e-08 as opposed to 1e-06 obtained in [25]. A load-classifying neural networks in [6] was also benchmarked, and it was seen that while it had an average error rate of 3.8 %, the proposed wide-FFNN model had an average error rate of less than 1 %.

3. Method

Estimating the SOC using a data-driven method first involves sourcing an appropriate dataset that contains the predictors of SOC derived from a standardized experimental exercise of the Lithium-ion battery. The LG 18650HG2 Li-ion Battery Dataset [26] consists of measurements from a 3 Ah LG HG2 cell tested in a thermal chamber with a 75amp, 5-volt Digatron Firing Circuits Universal Battery Tester channel with a voltage and current accuracy of 0.1 % of full scale. The battery is a Li [NiMnCo]O2 (H-NMC)/Graphite + SiO battery with a nominal voltage of 3.6 V, fast and normal charge current (CC-CV) of range 1.4 A, 4 A, 4.2 A, 50 mA and 100 mA respectively. The parameters/features in the data set consist of Time (time in seconds), Time Stamp (timestamp in MM/DD/YYYY HH:MM: SS AM format), Voltage (measured cell terminal voltage), Current (measured current in amps), Ah (measured amp-hours, with Ah counter, typically reset after each charge, test, or drive cycle), Wh (measured watt-hours, with Wh counter reset after each charge, test, or drive cycle), Power (measure power in watts), Battery_Temp_degC (battery case temperature, at the middle of battery, in degrees Celsius measured with an AD592 +/-1degC accuracy temperature sensor). Four pulse discharge HPPC tests were carried out at six (6) different temperatures (1, 2, 4, and 6C discharge and 0.5, 1, 1.5, and 2C charge, with reduced values at lower temperatures), 0.5C, 2C, and two 1C discharge tests, series of four - eight drive cycles performed, in the following order: UDDS, HWFET, LA92, and US06. The drive cycle power profile was then calculated for a single LG HG2 cell in a compact electric vehicle with all experimental data expressed in combined normalized forms. The combined normalized data for all resulting parameters is shown in Fig. 2.

3.1. State of charge (SOC) estimation methods

Linear regression is first considered for use in the estimation of state of charge (SOC) in this study. It is defined based on the simple regression model in Eq. (2), which relates one predictor to another.

$$y_i = b_o + \sum_{j=1}^{p} b_j x_{ij} + e_i \tag{2}$$

where, $i \in \{1, \ldots\ldots, n\}$, $y_i \in \mathbb{R}$ is the real-value response for the i-th observation, $b_o \in \mathbb{R}$, is the regression intercept, $b_j \in \mathbb{R}$, is the j-th predictor's regression slope, $x_{ij} \in \mathbb{R}$, is the j-th predictor for the i-th observation and the Gaussian error term is defined using Eq. (3):

$$e_i \sim N(0, \sigma^2) \tag{3}$$

The decision tree is another model considered for predicting the state of charge (SOC) of a Lithium-ion battery in this study. It is a hierarchical structure that consists of nodes connected by edges [27], where entropy typically determines the measure of impurity or the heterogeneity of each node.

Decision trees are built top-down starting from a root node. It involves data partitioning of subsets into homogenous instances. Standard deviation is then used to estimate the homogeneity of an estimated numerical sample with the mean square error (MSE) being a related metric for consideration.

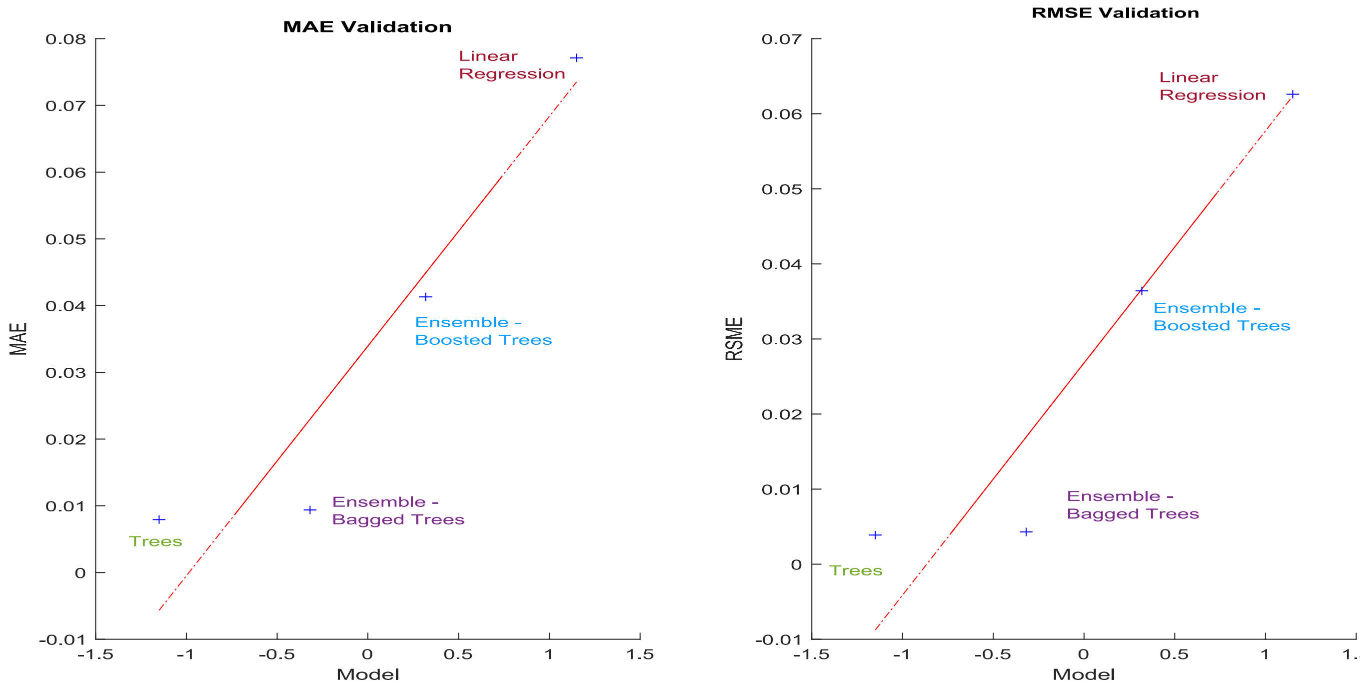

Fig. 4. RMSE and MSE comparison for the different models (training data).

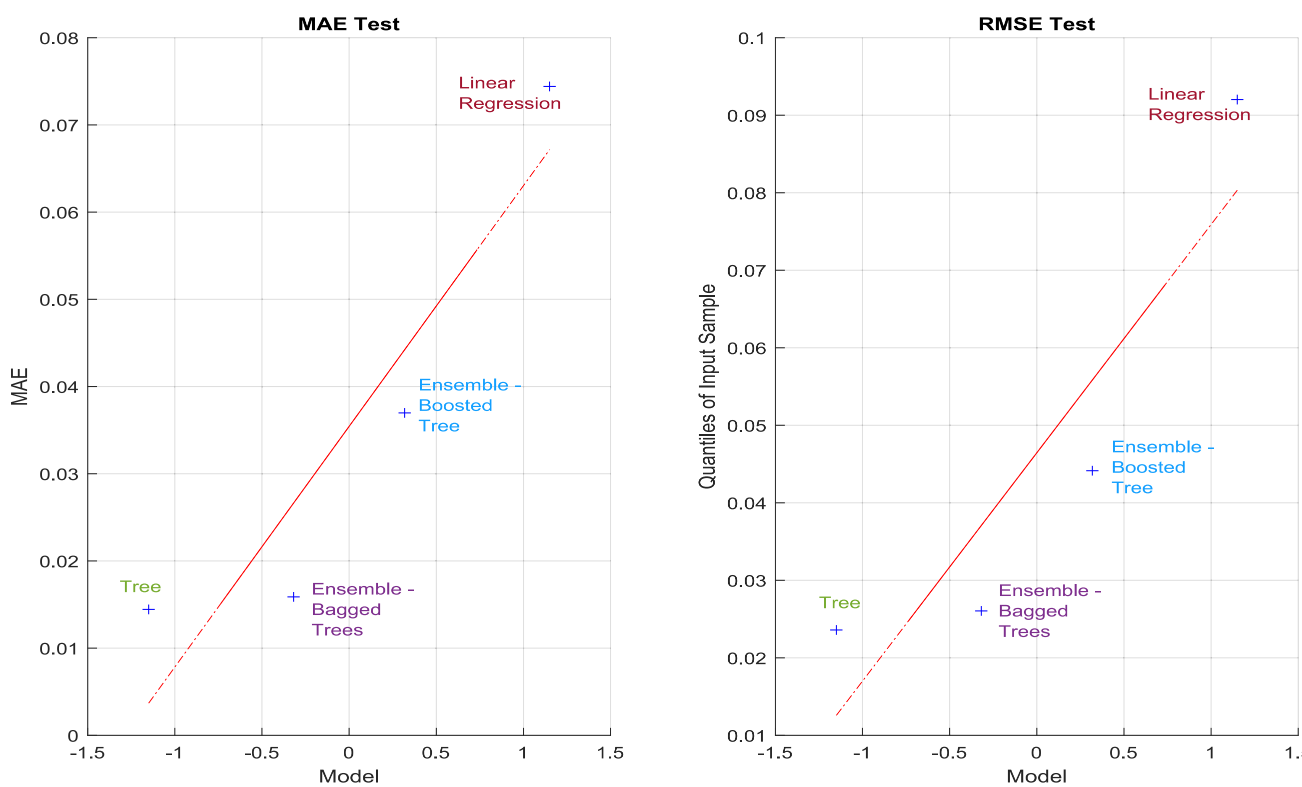

Fig. 5. RMSE and MSE plots for the different models (test data).

$$MSE = \frac{1}{n}\sum_{i=1}^{n}(y_i - \hat{y}_i)^2 \tag{4}$$

y_i is the actual value of the measurement and $\hat{y}_i$ is the prediction/predicted value of the measurement. Trees try to reduce the mean square error (MSE) at each child node rather than the entropy and this is a clear difference between regression and classification trees.

Neural networks are the third model considered in this study for estimating the SOC of a Lithium-ion battery (Fig. 3). Neural networks with an activation function, are deemed to have an equivalence and not an approximation to a decision tree [28].

State of Charge (SOC) is thus estimated in a neural network in line with the expression in Eq. (5),

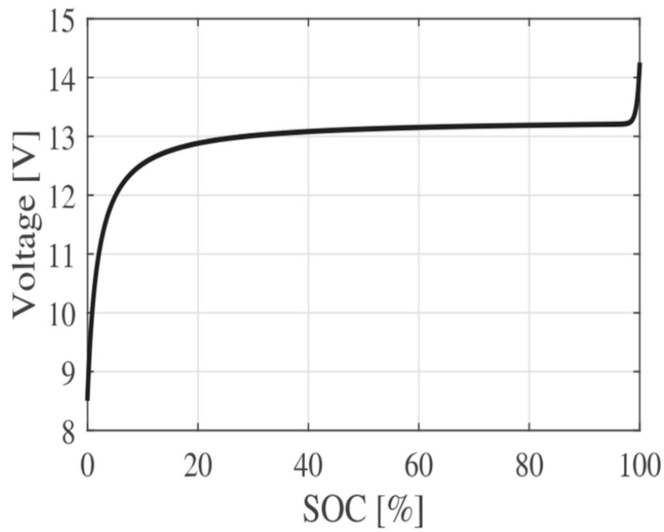

Fig. 6. OCV as a function of state of charge [32].

$$SOC = T\left[\sum_{K} W_j, k \times O_j + \theta_j, K\right] \tag{5}$$

where W_j,k, θ_j, K all denote the bias and weights from the hidden layer to the output layer respectively. The output of the output layer is denoted by O_j and T refers to the activation function deployed in the neural network. When the ANN has multiple layers between the input and the output layers, then such a network is regarded as a deep neural network (DNN) [30]. Deep neural networks have long demonstrated that they could model complex non-linear relationships, where different DNN architectures can generate compositional models of objects expressed as a layered composition of primitives [30]. Common DNN algorithms are the recurrent neural networks (RNN) primarily used for language modeling [31], long-short-term memory (LSTM) neural networks are also particularly effective for the same purpose, while convolutional neural networks (CNN) are commonly used in computer vision and imaging applications. The activation functions that are considered for the different layers in the neural network due to being monotonic, and differentiable would be the sigmoid as per Eq. (6), the Tanh as per Eq. (7), and the ReLU as per Eq. (8) respectively.

$$\varnothing(\mathrm{z}) = \frac{1}{1 + \mathrm{e}^{-\mathrm{z}}} \tag{6}$$

$$f(x) = tanh(z) = \frac{2}{1 + e^{-2z}} - 1 \tag{7}$$

$$\mathrm{R(Z)} = Max\ (0, \mathrm{z}) \tag{8}$$

The estimated SOC values by the different predictive models to be applied in this study would be compared with their real values using the maximum standard error (MSE), mean absolute error (MAE), and the root mean square error (RMSE) as per Eqs. (4), (9) and (10) respectively.

$$RMSE = \sqrt{\frac{1}{n}\sum_{i=1}^{n}(y_i - \hat{y}_i)^2} \tag{9}$$

$$MAE = \frac{1}{n}\sum_{i=1}^{n}|y_i - \hat{y}_i| \tag{10}$$

The real values (y_i) refer to the SOC values estimated in the LG 18650HG2 Li-ion Battery dataset used in training the model, while the predicted values $(\hat{y}_i)$ refers to the output values obtained during the data predictive estimation of different modeling techniques. MATLAB software and a personal computer with a core i7 CPU were used in system training and testing. The data from the dataset was already in normalized form (−1, 1) as observed in Fig. 2, 70 % of the data was used for training, while 30 % was used for testing for the neural network models, linear regression models, and the regression tree models.

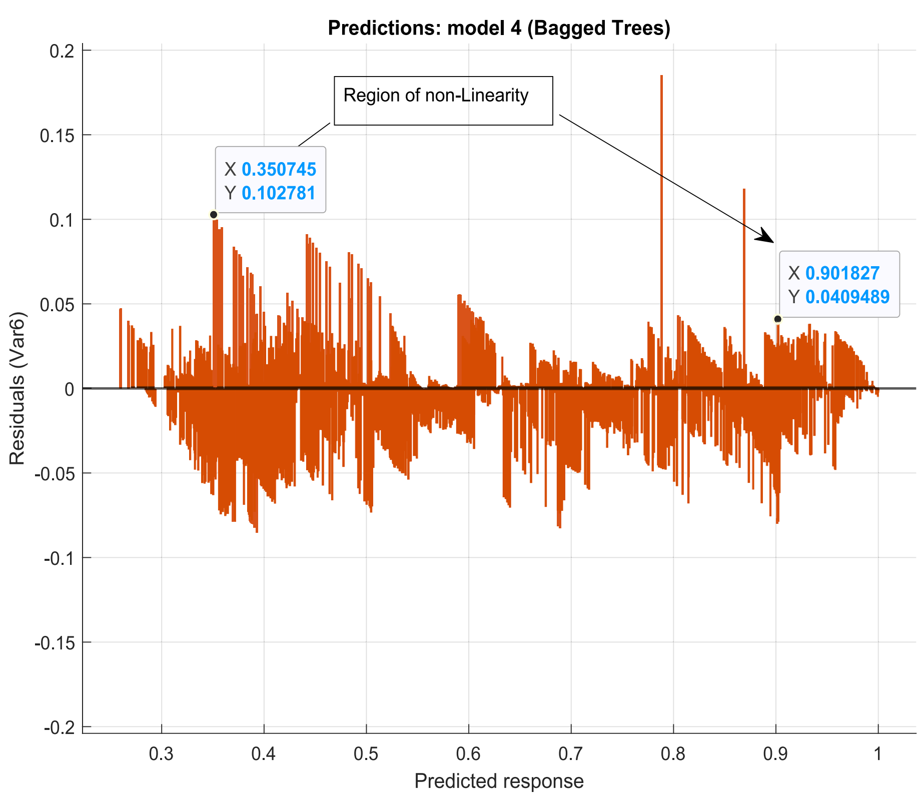

Fig. 7. Residual of predicted response.

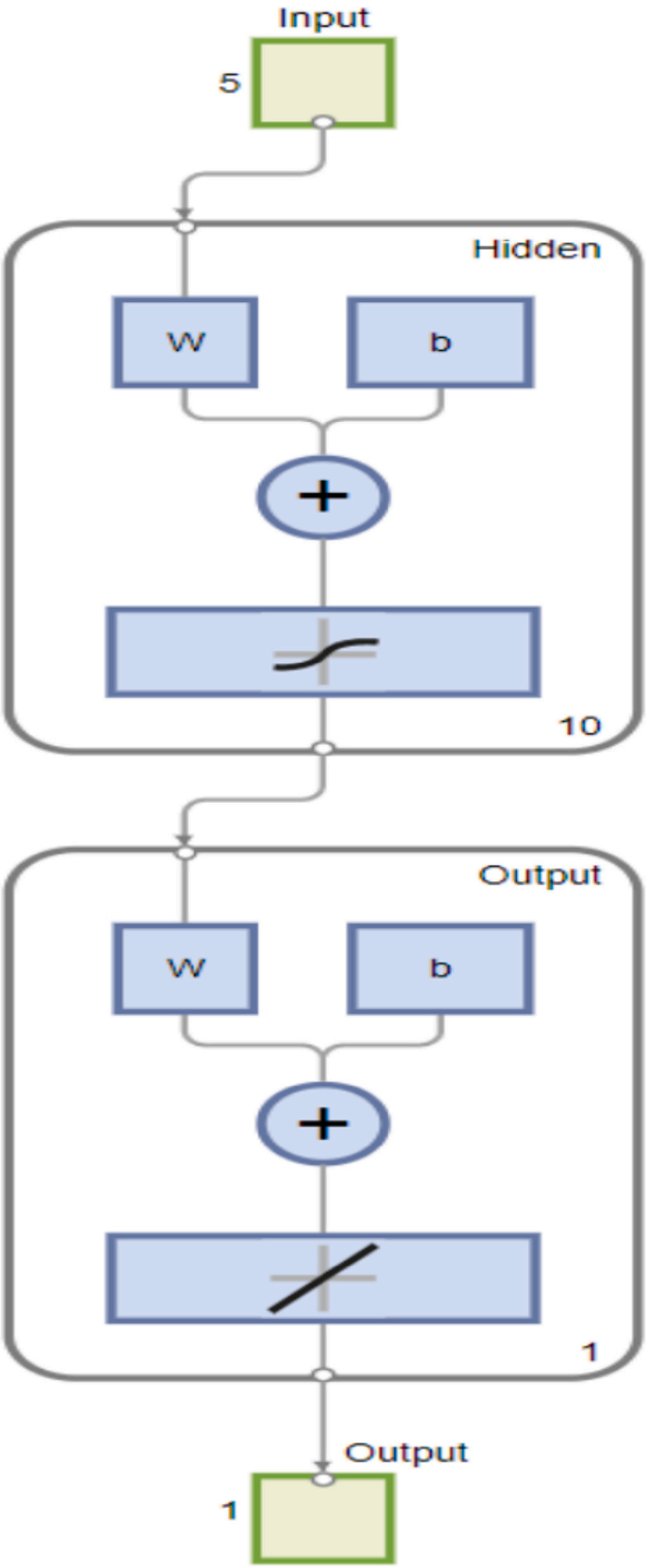

Fig. 8. Single layer FFNN.

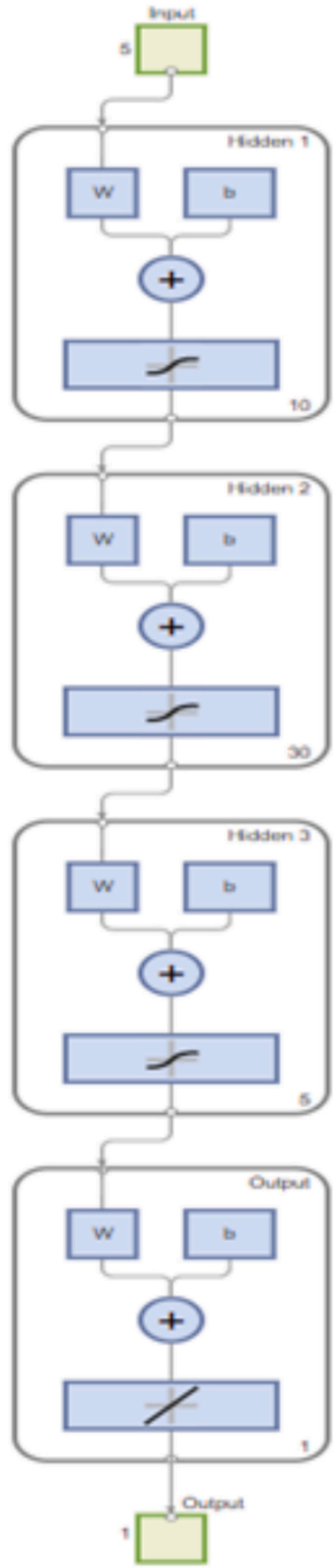

Fig. 9. Tri-layered neural network.

4. Result and discussion

4.1. SOC estimation using linear regression and regression trees

Five (5) cross-fold validation was used in the models to ensure an easy assessment of the model performance was possible while ensuring

Table 2
Training results for model on dataset.

Training					
Model	Activation function	MAE	MSE	RMSE	R-squared
Narrow neural network	ReLU	0.014677233	0.000596285	0.024418942	0.994627014
	Tanh	0.014601409	0.000599853	0.024491895	0.994594862
	Sigmoid	0.015107251	0.000623069	0.024961358	0.994385663
Medium neural network	ReLU	0.012842963	0.000514496	0.022682511	0.995363991
	Tanh	0.014153716	0.00057365	0.023950991	0.994830971
	Sigmoid	0.01525317	0.000625499	0.025009978	0.994363771
Wide neural network	ReLU	0.011080935	0.000453449	0.021294351	0.995914071
	Tanh	0.014824104	0.000601364	0.024522724	0.994581246
	Sigmoid	0.015912847	0.000675248	0.025985533	0.993915495
Bi-layered neural network (FFNN)	ReLU	0.01240777	0.000500136	0.022363713	0.995493391
	Tanh	0.013362049	0.000544578	0.023336186	0.995092935
	Sigmoid	0.015265527	0.000623625	0.024972478	0.99438066
Tri-layered neural network (FFNN)	ReLU	0.012048151	0.000489752	0.022130348	0.995586953
	Tanh	0.013001267	0.000525526	0.022924345	0.995264608
	Sigmoid	0.015087228	0.000622973	0.024959418	0.994386536

Table 3
Testing results for model on dataset.

Testing					
Model	Activation function	MAE	MSE	RMSE	R-squared
Narrow neural network	ReLU	0.013104009	0.000289125	0.017003677	0.995268057
	Tanh	0.011522578	0.000240913	0.01552138	0.996057111
	Sigmoid	0.011459703	0.000255885	0.015996406	0.995812077
Medium neural network	ReLU	0.011909586	0.000265727	0.01630114	0.995650995
	Tanh	0.011226793	0.000230147	0.015170582	0.996233323
	Sigmoid	0.013138933	0.000315092	0.017750818	0.994843078
Wide neural network	ReLU	0.009008496	0.000165083	0.012848447	0.997298188
	Tanh	0.012908862	0.000294475	0.017160276	0.995180495
	Sigmoid	0.013941495	0.000345229	0.018580335	0.994349837
Bi-layered neural network (FFNN)	ReLU	0.011390927	0.000269233	0.016408312	0.995593622
	Tanh	0.011919245	0.00024363	0.01560864	0.996012653
	Sigmoid	0.01427445	0.000358725	0.018940031	0.994128957
Tri-layered neural network (FFNN)	ReLU	0.009867597	0.000189458	0.013764363	0.996899255
	Tanh	0.010050675	0.000198091	0.014074471	0.996757962
	Sigmoid	0.014246918	0.000367847	0.01917933	0.993979664

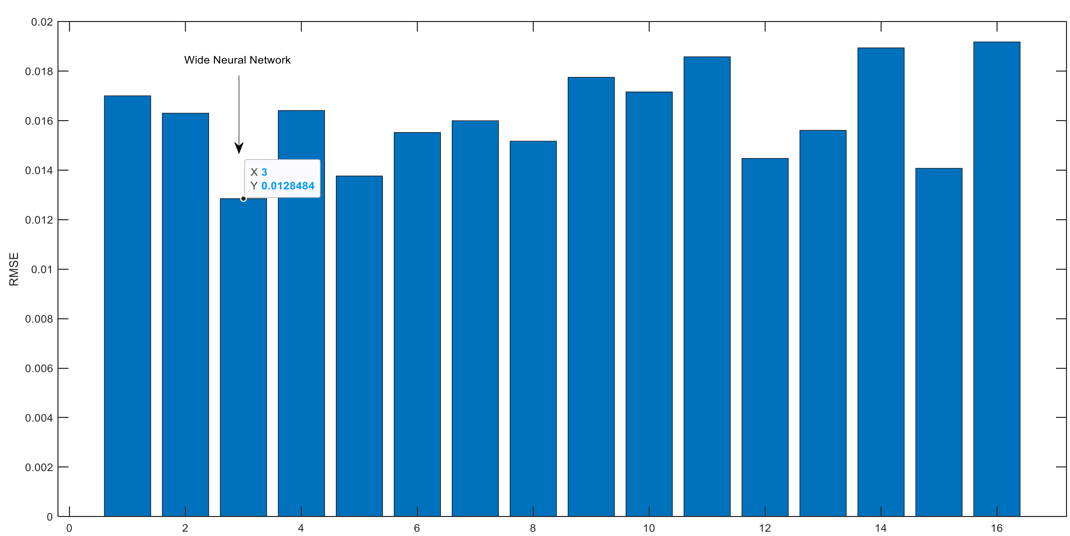

Fig. 10. Comparison amongst all trained and tested neural network models.

robustness and bias minimization. This is particularly useful since the train-test split method was being used in all cases. The robust option for the linear regression model was not selected and a regression tree, as well as its ensemble variants of bagged trees and boosted trees were selected for training. Principal component analysis (PCA) was disabled for all models as optimization for each model was not being considered at this stage. Minimum leaf sizes of 8 and 30 learners were adopted for each tree and a learning rate of 0.01 was used in the boosted ensemble regression tree. Table 1 depicts the MAE, MSE, and RSME obtained for the different machine-learning models.

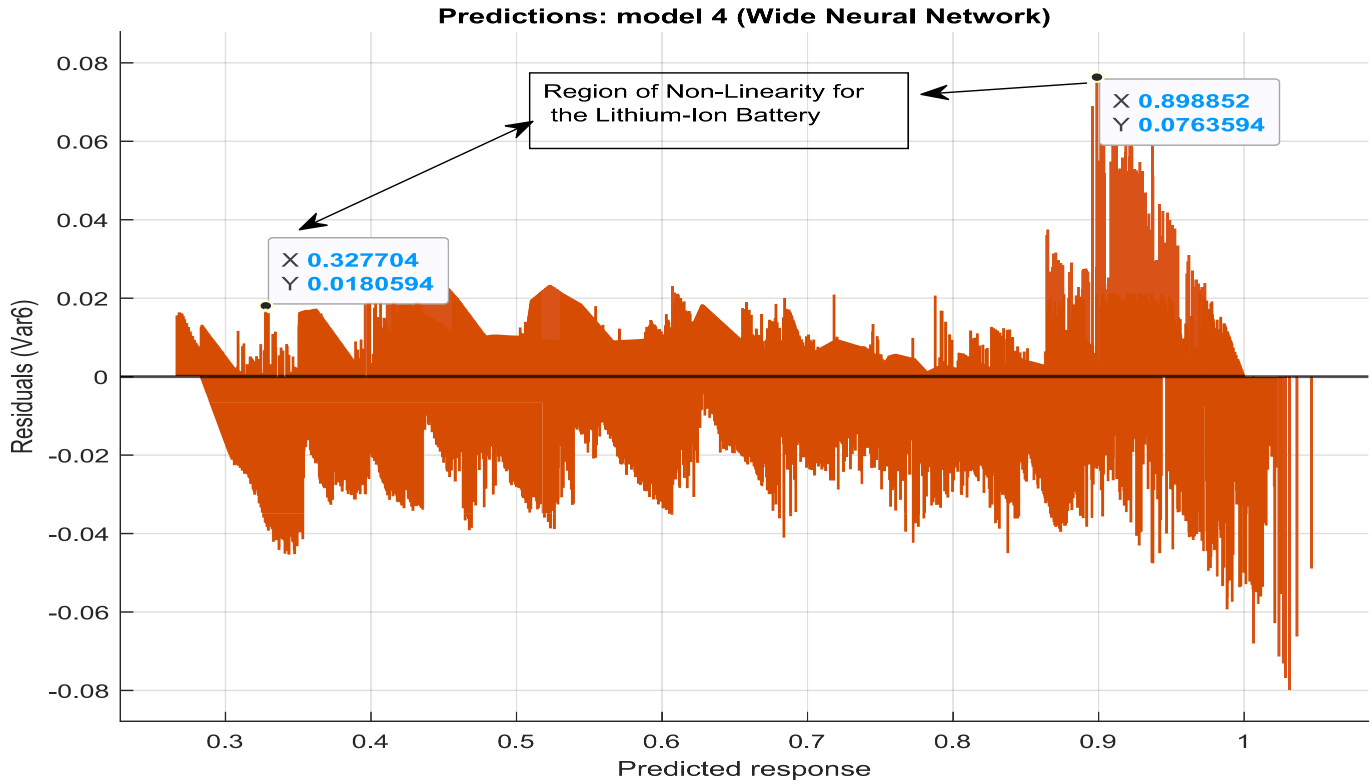

Fig. 11. Residual plot of predicted response for the wide neural network.

Table 4
Training and testing results for FFNN (tri-layered).

Model	Parameters	MAE	MSE	RMSE	R-squared
Training					
Tri-layered neural network (FFNN)	ReLU, layer sizes (100:100:100), 1500 epoch	0.009437887	0.000389889	0.019745604	0.9964868
Tri-layered neural network (FFNN)	ReLU, layer sizes (100,200,100), 2000 epochs	0.008860954	0.000350872	0.018731588	0.996838369
Tri-layered neural network (FFNN)	ReLU, layer sizes (100:100:100), 1000 epochs	0.009856033	0.000414515	0.02035964	0.9962649
Testing					
Tri-layered neural network (FFNN)	ReLU, layer sizes (100:100:100), 1500 epochs	0.010097748	0.000223275	0.014942393	0.996345784
Tri-layered neural network (FFNN)	ReLU, layer sizes (100,200,100), 2000 epochs	0.00948967	0.000210216	0.014498819	0.996559519
Tri-layered neural network (FFNN)	ReLU, layer sizes (100:100:100), 1000 epochs	0.009546607	0.000186722	0.013664617	0.996944032

The four models examined with performance values detailed in Table 1, Figs. 4, and 5 respectively show that they can all be used to estimate the SOC of a lithium-ion battery with an MAE in the range of 0.032948 to 0.0044787, an MSE in the range 0.0000734553 to 0.0019538, and an RMSE in the range 0.0085705 to 0.044202 during the training phases, while in the test phase, the MAE is in the range 0.014091 to 0.036976, the MSE is in the range 0.00052991 to 0.0020742 and the RMSE is in the range 0.02302 to 0.045543 respectively. Ensemble bagged trees have the best performance with an RSME of 0.0085705, MSE of 0.0000734553 in the training phase, an RMSE of 0.02302, and MSE of 0.00052991 in the test phase. The bagged ensemble tree model performed better in this case because bagging attempts to reduce the chance of overfitting the complex models, enhancing prediction stability through the aggregation of multiple regressor outputs. This is evidenced in the model's improved performance on the test set, which demonstrates how bagged trees could capture a battery's non-linear dynamic performance while retaining past information. While the bagged tree (ensemble) is a good model, there still exists concerns about a vast difference in training and testing metrics for the model, it would likely not be great in practical applications due to high residuals (errors) occurring within the non-linear open circuit voltage (OCV) range (20 % SOC and 80–90 % SOC) of a typical lithium-ion battery as seen in Figs. 6 and 7 respectively.

4.2. *SOC estimation using neural networks*

The Neural networks shown in Figs. 8 and 9 respectively are trained and tested with the dataset, where Tables 2 and 3 represent the details of their performance under varying activation conditions (ReLU, Tanh, and Sigmoid).

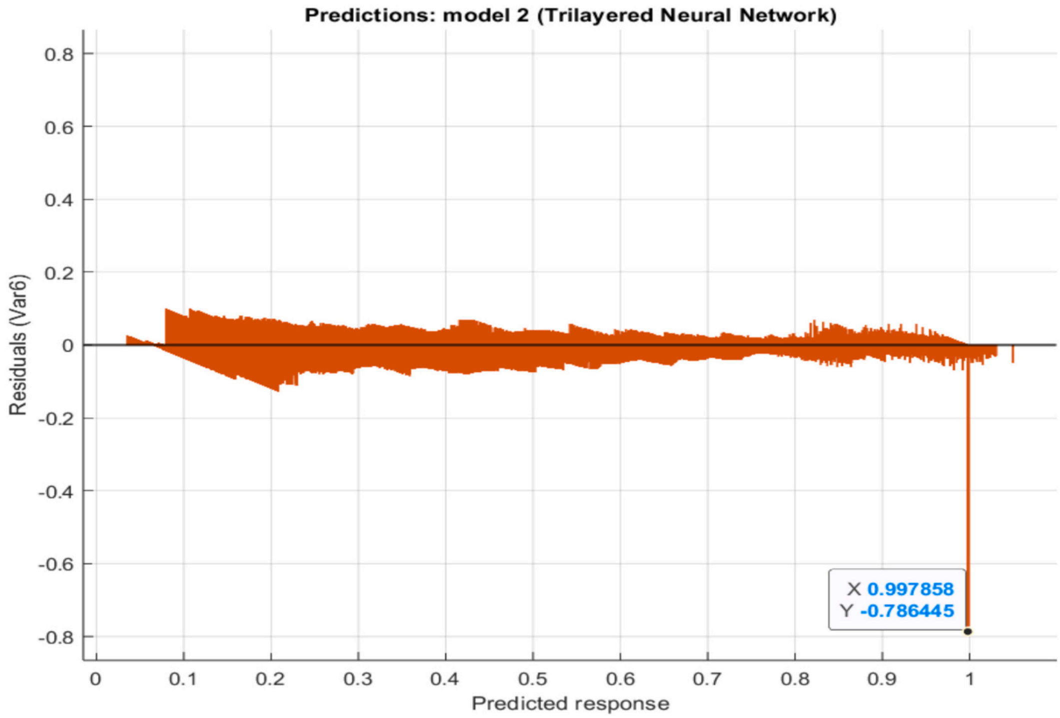

Fig. 12. Residual plot for tri-layered network.

Algorithm 1. Training algorithm.

1: Procedure BACK PROPAGATION (D, n)
2: Load Training Set, D = (x, y), where k =1, learning rate (n)
3: Initialize FFNN weights to H_0
4: Model Initialization
5: While Early stopping Patience <= 15, do
6: For $((x^p, y^p) \in D$
7: Compute y_j^p
8: Compute δ_β^p
9: Compute δ_α^q
10: Compute w_q^p
11: N = 0.1 * n.

The input to the neural network is a vector $X = [V_k, I_k, T_k]$, which denotes the combined battery normalized voltage, combined battery normalized current, and temperature respectively as depicted in Fig. 2, while $Y = SOC_k$. The input vector is fed to the input of the FFNN, and the output is the SOC. To yield Y_k, the input X_k is multiplied many times using matrix multiplication, where the activation for each layer (h) is estimated as

$$h_g^l = \sigma\left(\sum\left(w_{f,g}^l h_g^{l-1} - b_g^l\right)\right) \quad (11)$$

where w^l denotes the weights on each layer (l), σ^l denotes the activation of layer (l), and b^l denotes the bias in each layer (l). The activation functions defined in Eqs. (6), (7), and (8) relating to the Tanh, Sigmoid, and ReLU activations are applied to the different layers of the FFNN and the training result in each case as seen in Table 2.

The narrow neural network with a first layer size of 10 processing units and one fully connected layer at a maximum epoch size of 1000 was trained and tested with the ReLU, Tanh, and Sigmoid activation functions respectively with MAE in the range of 0.014601409 to

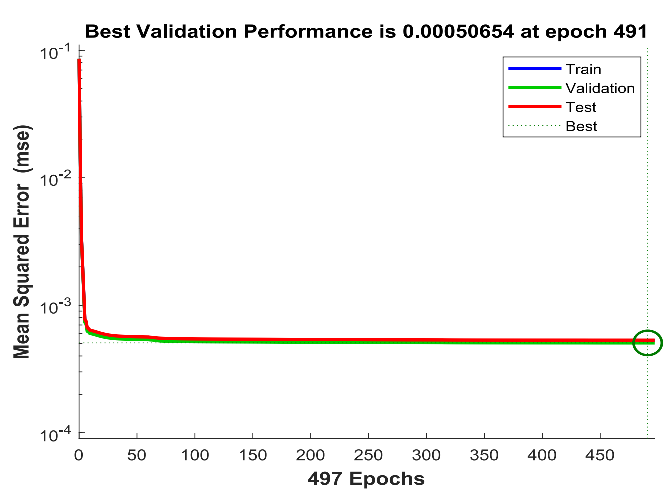

Fig. 13. Single layer FFNN validation performance.

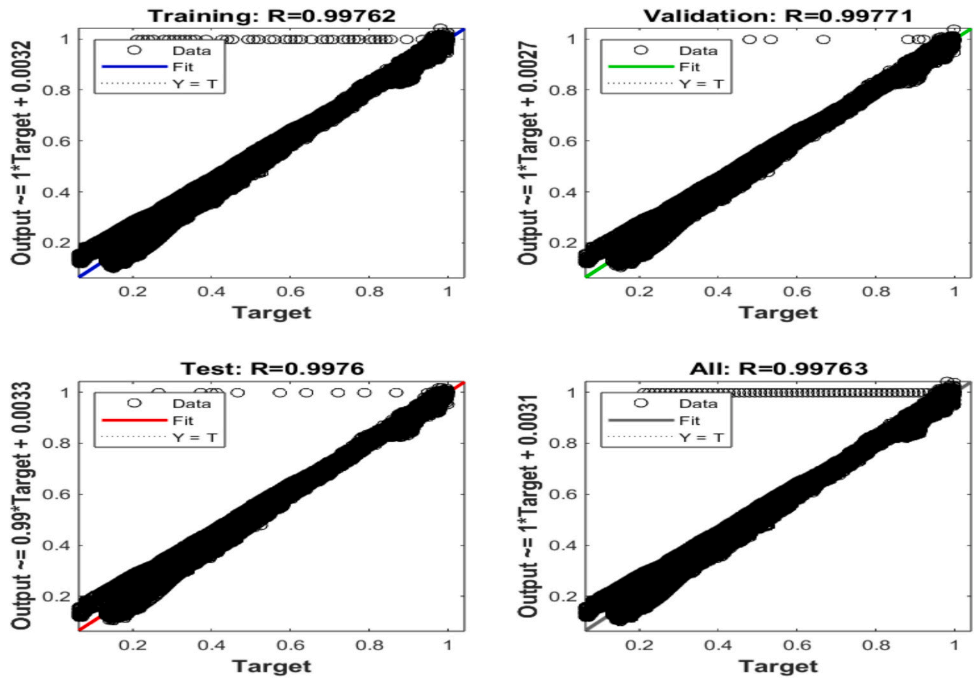

Fig. 14. Single layer FFNN training and test performance.

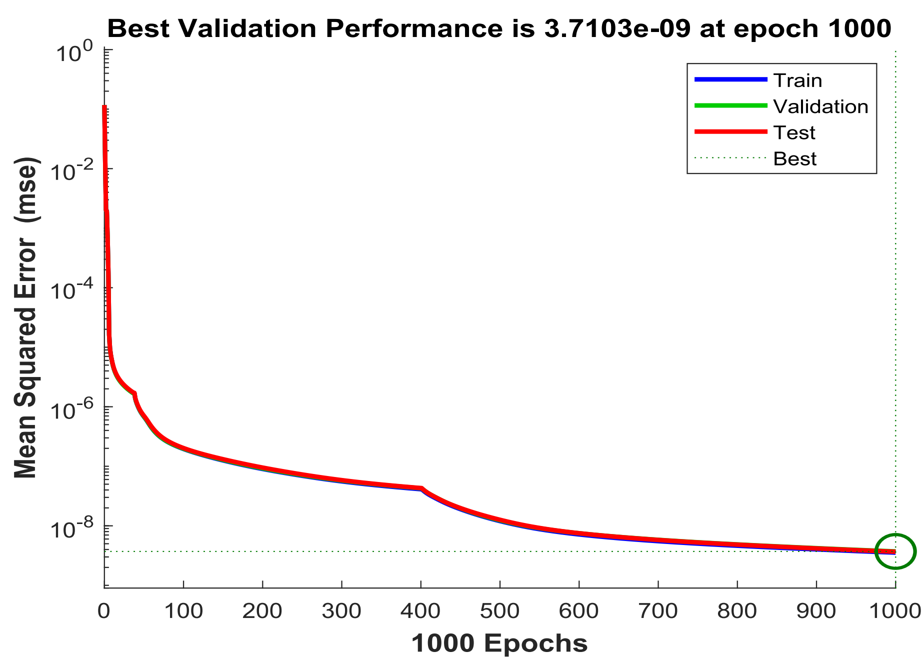

Fig. 15. 3-Layer FFNN validation performance.

0.015107251 in training, and 0.011459703 to 0.013104009 in the test phase, MSE in the range 0.000596285 to 0.000623069 in training, and 0.000240913 to 0.000289125 in testing, and RMSE in the range 0.024418942 to 0.024961358 in training, and 0.01552138 to 0.017003677 in testing phase, where the most accurate of them was the narrow neural network with the Tanh activation function, with an MSE of 0.000240913 and RMSE of 0.01552138.

The first layer size was increased to 25 with a single fully connected layer to generate a medium neural network, which was also trained and tested at a maximum epoch of 1000 with the ReLU, Tanh, and Sigmoid activation functions respectively. This has an MAE in the range 0.012842963 to 0.01525317 in the training phase, 0.011226793 to 0.013138933 in the test phase, MSE in the range 0.000514496 to 0.000625499 in training, and 0.000230147 to 0.000315092 in testing, and RMSE in the range 0.022682511 to 0.025009978 in training, and, 0.015170582 to 0.017750818 in testing. Where the most accurate was the Medium Neural Network with a Tanh activation function, with an MSE of 0.000230147 and RMSE of 0.015170582. The result obtained demonstrated that the Tanh activation function provided good accuracy for a single-layer neural network with a small to medium number of processing elements.

A further increase was made to the first layer size to realize an increment of 100 with a single fully connected layer to generate a wide neural network, which was trained and tested at a maximum epoch of

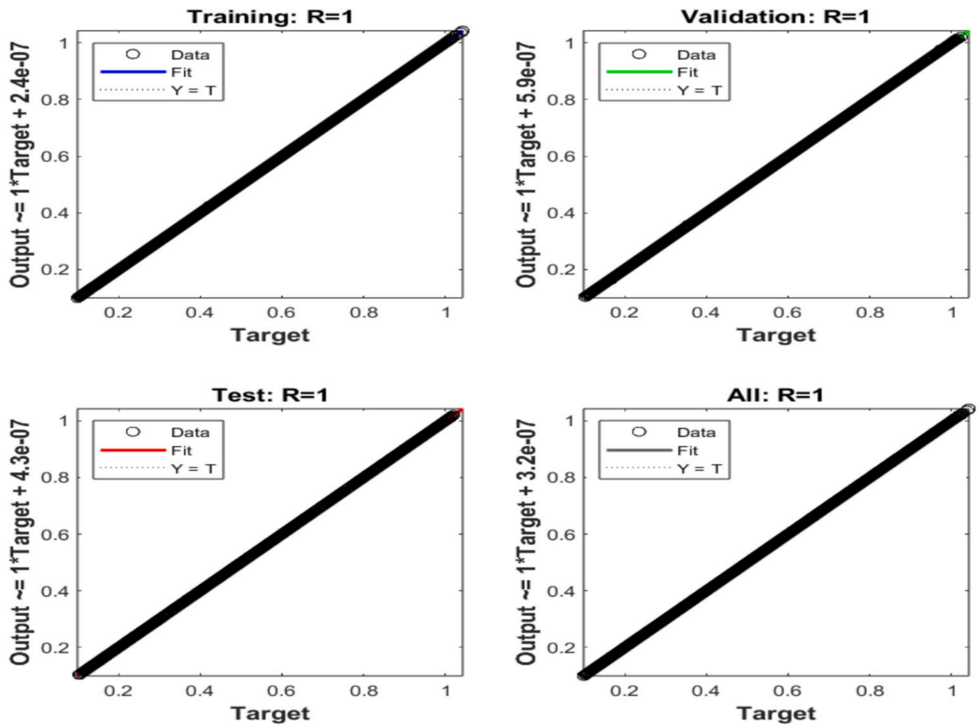

Fig. 16. 3-Layer FFNN training and test performance.

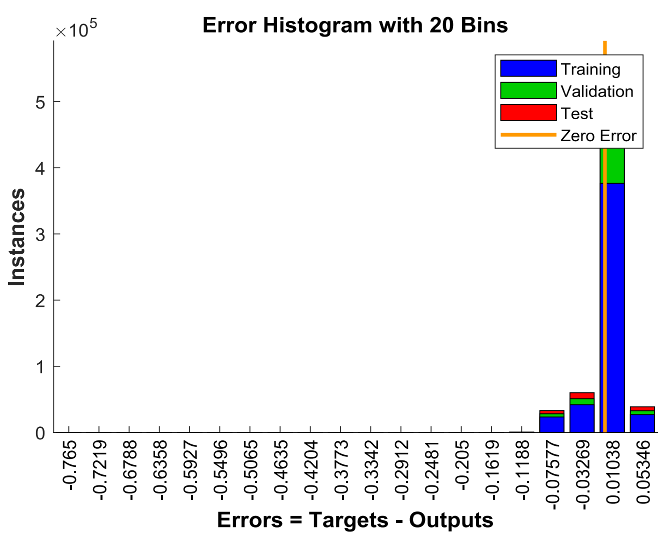

Fig. 17. Error histogram of single-layer FFNN.

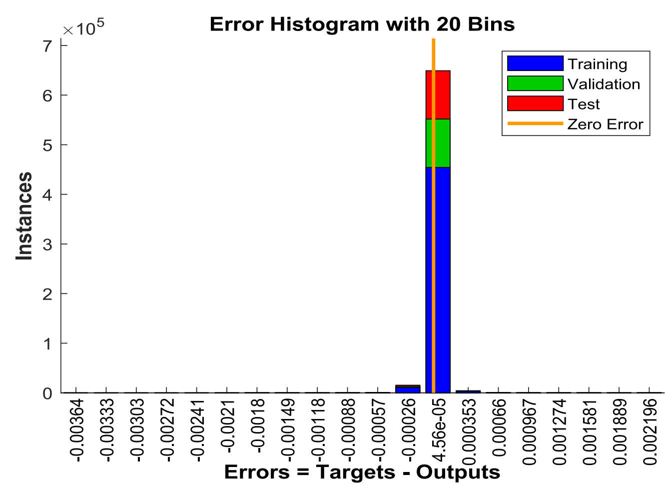

Fig. 18. Error histogram of 3-layered FFNN.

1000 with the ReLU, Tanh, and Sigmoid activation functions respectively. This has an MAE in the range 0.011080935 to 0.015912847 in training, 0.009008496 to 0.013941495 in testing, MSE in the range 0.000453449 to 0.000675248 in training, and 0.000165083 to 0.000345229 in testing, and RMSE in the range 0.021294351 to 0.025985533 in training, and 0.012848447 to 0.018580335 in testing. The most accurate was the wide neural network with the ReLU activation function, with an MSE of 0.000165083 and RMSE of. 0.012848447.

A Feedforward neural (FFNN Bi-layered) network with two fully connected layers, each of its two hidden layers with ten processing units, was trained and tested at 1000 epochs with the ReLU, Tanh, and Sigmoid activation functions respectively. These gave an MAE in the range of 0.01240777 to 0.015265527 in training, and 0.011390927 to 0.01427445 in the test phase, an MSE in the range of 0.000500136 to 0.000623625 in the training phase, and 0.00024363 to 0.000358725 in the test phase, an RMSE in the range 0.022363713 to 0.024972478 in training, and 0.01560864 to 0.018940031 in testing. Where the most accurate was the Bi-layered Neural Network (FFNN) with a Tanh activation function, with an MSE of 0.00024363, and RMSE of 0.01560864. It should be noted that the Bi-Layered neural network with a ReLU activation function, had a better performance/accuracy during the training phase of the model. Thus, a Tri-layered network with three fully connected layers, where each of the three layers had ten processing units respectively was trained and tested at 1000 epochs with the ReLU, Tanh and Sigmoid activation functions respectively. Where the most accurate was the tri-layered neural network (FFNN) with ReLU activation function, with an MSE of 0.000189458, and RMSE of 0.013764363. Upon Comparison between all the models, it is observed that the wider the neural network, the more accurate its prediction of the state of charge (SOC). Fig. 10 depicts the RMSE plot for all tested models.

Table 5
Performance of different related SOC methods in discharge mode.

Method	Error	Error method	Reference
Kalman filter (UKF)	1.05 %	MAE	[34]
Kalman filter (CDKF)	0.96 %	MAE	[34]
Particle filtering (PF)	0.2 %	MAE	[34]
Kalman filter (AEKF)	7.26 %	MAE	[35]
Adaptive particle filtering (APF)	4.62 %	MAE	[35]
Proposed FFNN (wide)	0.88 %	MAE	
Deep neural network (DNN)	1.10 %	MAE	[36]
Convolutional neural network (CNN-UNET)	1.5 %	MAE	[37]
Long short-term memory (LSTM)	2.36 %	MAE	[38]
LSTM-AHIF	1.18 %	MAE	[38]
Recurrent neural network (RNN)	2.50 %	MAE	[39]
GRU-RNN	2.53 %	MAE	[39]
DAE-GRU	1.59 %	MAE	[39]

The wide area neural network is compared with the bagged trees response in the previous analysis, where the residuals generated as depicted in Figs. 7 and 11 respectively, show that the bagged trees had a residual range of −0.09 to 0.19, while the wide neural network had a residual range of −0.05 and 0.079 all lying within the non-linear OCV range for a lithium battery. The wide neural network is thus deemed to outperform the bagged trees model.

However, the wide area network could still be improved by adding more layers to it and utilizing the ReLU activation function, which has so far demonstrated its ability to outperform the Tanh and Sigmoid functions. Thus, a wide Tri-layered feed-forward neural network was trained and tested on the same dataset with training and test results shown in Table 4.

The neural network was made wide with a minimum of 100 processing elements in each layer and training for more than 1000 epochs (1500 and 2000 respectively). The model with the best performance in the training and test phases was the Tri-layered feed-forward neural network with MSE of 0.000350872 and 0.000186722, and RMSE of 0.018731588 and 0.013664617 respectively. These indicate the impact of having many processing units in the neural network and how the ratio of these impacts the obtained result. In the training phase, the network training at 2000 epochs with a 1:2:1 number of processing elements performed better, however, in the test phase, the wide area network had better performance and produced residuals ranging between −0.1 and 0.1 as shown in Fig. 12. The wide network depicted in Fig. 9, still outperformed the Tri-layered network, thus showing that for the prediction of the state of charge of lithium-ion batteries, the wider the neural networks rather than its depth (deep neural networks), the more accurate the model will be for fault detection in battery management systems.

4.3. Model validation

The validation of the single-layer FFNN and a Tri (3)-layer feed-forward neural network are shown in Figs. 13, 14, 15, and 16, respectively with varying activation functions applied at each layer (Tanh &Sigmoid -Hidden, and in the ReLU - Output) with simulated test data. The results are:

The single-layer FFNN converged after 491 epochs, with an MSE of 0.00050654. However, the entire prediction had an error bias of 0.0031, as seen in Fig. 13. The FFNN was extended to three (3) layers and its performance is depicted in Figs. 15 and 16.

The three-layer FFNN was able to achieve some convergence at 1000 epochs, which took a far longer time to train the model as opposed to a single-layer FFNN. However, it can be clear that it has an MSE of 3.7103e-09. Both network models had acceptable R-squared values of above 0.99 in each case (training and testing). The key feature for State of charge prediction is measured by the ability of a model to achieve some accuracy within the non-linear range of the Li-ion battery, which can be seen in Fig. 6. Which shows the open circuit voltage (OCV) relationship with the state of charge of a Li-ion battery, between 20 % SOC and 93 % SOC there exists a non-linear relationship and this is where the estimation of SOC poses challenges. While the SOC is reducing, the open circuit voltage (OCV) tends to remain constant, till SOC drops below 20 %. The FFNN was able to accurately model and predict the SOC for the entire data range except at the higher values of 100 % in the dataset for the single layer FFNN as seen in Fig. 12.

The Error histograms for the single-layer and 3-layer FFNN are seen in Figs. 17, and 18, respectively.

5. Conclusion

Battery management systems are designed to not only manage the operations of the battery pack providing power to a system (electric vehicles, autonomous robots, etc.), but to also provide a means for early detection of faults in the battery system. State of charge estimation provides a simple metric for estimating the state of health of a battery-powered system. However, the estimation of SOC is itself a challenge occasioned by the open circuit voltage (OCV) characteristics of a lithium-ion battery in charge and discharge conditions. Data-driven solutions utilizing neural networks have been long considered and utilized for this estimation, however, much focus has been placed on the depth of the neural network, and while deep neural networks offer a good solution to SOC estimation there is an absence of works to support or validate its choice nor the ability for the simple feed-forward neural network to offer competitive performance. This study demonstrates the ability of the simple linear regressor, ensemble methods (boosted and bagged trees), and various neural network structures to estimate their predictive ability on a known dataset. While all the models were able to predict the SOC with varying degrees of accuracy, it was observed the bagged trees ensemble model outperformed all other considered models, in comparison with neural networks, it was observed from the results obtained that neural networks are the ideal candidate for such predictions as opposed to linear regressors or ensemble regressors (trees). Amongst the neural networks selected, it was observed that the network had high accuracy and minimal residuals when it was made wider instead of deeper (more than 3 layers). The more processing units adopted at each layer, the better the performance of the network. To further prove this, multilayered feed-forward neural networks were made wider, with more processing units added, and trained at higher epoch values of 1500 and 2000 respectively.

The performance of the FFNN model was compared to different models as seen in Table 5. The MAE metric was used to consider related studies, and all studies were estimated using battery datasets representing discharge operating mode. The proposed model was only outperformed by the particle filtering method, which is understandable as the dataset used in that study was not as large as that used in this study, and particle filtering is an optimization model. However, in-depth analysis revealed that the more mainstream methods such as various variants of the Kalman filter had a best performance of 0.96 % at the low end and 7.26 % on the high end, DNN and CNN had error rates of 1.1 % and 1.5 % respectively, while recurrent neural networks and some variants of it had error percentages ranging from 1.59 % on the low end to 2.50 % on the high end. These all represent good to acceptable performances for the neural network in which the worst-performing models outperformed the linear regression and ensemble methods also considered in this study. However, the results obtained in this study provide a definite answer in the author's opinion as to what is the optimal number of layers to apply to an FFNN for SOC estimation, which was established at three (3), at 1000 epochs. There was no significant improvement when the number of layers was either increased or the epochs increased. While this report disagrees with the position established in [6] which stated that the number of nodes does not have any marked effect on the accuracy of the model, however, the result of this study shows that the wider the network (more nodes), the better the minimization of the loss function and overall accuracy. This can be seen also in the work using parallel neural networks to achieve a wide and powerful neural network in [33] which was used in battery pack state of charge estimation with an MSE of 0.0268 % which outperformed other models compared to combined operations SOC estimation.

The results of this study also demonstrated a marked improvement over the default neural network structure (single layer FFNN), which further justifies the position that while deep networks are good candidates for the estimation of SOC, wide feed-forward neural networks would also provide similar performance at less computational costs required for integration into thin clients of hardware such as the battery management system.

CRediT authorship contribution statement

Edward Ositadinma Ofoegbu: Writing – review & editing, Writing – original draft, Visualization, Validation, Supervision, Software, Resources, Project administration, Methodology, Investigation, Formal analysis, Data curation, Conceptualization.

Declaration of competing interest

The authors declare that they have no known competing financial interests or personal relationships that could have appeared to influence the work reported in this paper.

Acknowledgment

The author wishes to acknowledge the support (financial and Technical) received from the RDF development fund of Leeds Beckett University and the School of Built Environment, Engineering and Computing (engineering group).

Data availability

Data will be made available on request.

References

[1] K.W.E. Cheng, B.P. Divakar, H. Wu, K. Ding, H.F. Ho, Batterymanagement system (BMS) and SOC development for electrical vehicles, IEEE Trans. Veh. Technol. 60 (1) (Jan. 2011) 76–88.
[2] M.K. Loganathan, C.M. Tan, B. Mishra, T.A.M. Msagati, L.W. Snyman, Review and selection of advanced battery technologies for post 2020 era electric vehicles, in: 2019 IEEE Transportation Electrification Conference (ITEC-India), IEEE, 2019, pp. 1–5.
[3] Y. Xing, E.W.M. Ma, K.L. Tsui, M. Pecht, Battery management systems in electric and hybrid vehicles, Energies (Basel) 4 (11) (Oct. 2011) 1840–1857, https://doi.org/10.3390/en4111840.
[4] A. Vasebi, S.M.T. Bathaee, M. Partovibakhsh, Predicting state of charge of lead-acid batteries for hybrid electric vehicles by extended Kalman filter, Energy Convers. Manag. 49 (1) (2008) 75–82, https://doi.org/10.1016/j.enconman.2007.05.017.
[5] W. He, N. Williard, C. Chen, M. Pecht, State of charge estimation for Li-ion batteries using neural network modeling and unscented Kalman filter-based error cancellation, Int. J. Electr. Power Energy Syst. 62 (Nov. 2014) 783–791, https://doi.org/10.1016/j.ijepes.2014.04.059.
[6] S. Tong, J.H. Lacap, J.W. Park, Battery state of charge estimation using a load-classifying neural network, J. Energy Storage 7 (Aug. 2016) 236–243, https://doi.org/10.1016/j.est.2016.07.002.
[7] M.-H. Hung, C.-H. Lin, L.-C. Lee, C.-M. Wang, State-of-charge and state-of-health estimation for lithium-ion batteries based on dynamic impedance technique, J. Power Sources 268 (Dec. 2014) 861–873, https://doi.org/10.1016/j.jpowsour.2014.06.083.
[8] H. He, R. Xiong, J. Fan, Evaluation of lithium-ion battery equivalent circuit models for state of charge estimation by an experimental approach, Energies (Basel) 4 (4) (Mar. 2011) 582–598, https://doi.org/10.3390/en4040582.
[9] Z. Cui, L. Wang, Q. Li, K. Wang, A comprehensive review on the state of charge estimation for lithium-ion battery based on neural network, Int. J. Energy Res. 46 (5) (Apr. 2022) 5423–5440, https://doi.org/10.1002/er.7545.
[10] L. Kang, X. Zhao, J. Ma, A new neural network model for the state-of-charge estimation in the battery degradation process, Appl. Energy 121 (May 2014) 20–27, https://doi.org/10.1016/j.apenergy.2014.01.066.
[11] M. Ismail, R. Dlyma, A. Elrakaybi, R. Ahmed, S. Habibi, Battery state of charge estimation using an Artificial Neural Network, in: 2017 IEEE Transportation Electrification Conference and Expo (ITEC), IEEE, Jun. 2017, pp. 342–349, https://doi.org/10.1109/ITEC.2017.7993295.
[12] M.S. Hossain Lipu, M.A. Hannan, A. Hussain, A. Ayob, M.H.M. Saad, K.M. Muttaqi, State of charge estimation in lithium-ion batteries: a neural network optimization approach, Electronics (Basel) 9 (9) (Sep. 2020) 1546, https://doi.org/10.3390/electronics9091546.
[13] D. Jiménez-Bermejo, J. Fraile-Ardanuy, S. Castaño-Solis, J. Merino, R. Álvaro-Hermana, Using dynamic neural networks for battery state of charge estimation in electric vehicles, Procedia Comput. Sci. 130 (2018) 533–540, https://doi.org/10.1016/j.procs.2018.04.077.
[14] F. Yang, W. Li, C. Li, Q. Miao, State-of-charge estimation of lithium-ion batteries based on gated recurrent neural network, Energy 175 (May 2019) 66–75, https://doi.org/10.1016/j.energy.2019.03.059.
[15] W. He, N. Williard, C. Chen, M. Pecht, State of charge estimation for Li-ion batteries using neural network modeling and unscented Kalman filter-based error cancellation, Int. J. Electr. Power Energy Syst. 62 (Nov. 2014) 783–791, https://doi.org/10.1016/j.ijepes.2014.04.059.
[16] S. El Fallah, J. Kharbach, Z. Hammouch, A. Rezzouk, M. Ouazzani Jamil, State of charge estimation of an electric vehicle's battery using Deep Neural Networks: simulation and experimental results, J. Energy Storage 62 (Jun. 2023) 106904, https://doi.org/10.1016/j.est.2023.106904.
[17] D.N.T. How, M.A. Hannan, M.S.H. Lipu, K.S.M. Sahari, P.J. Ker, K.M. Muttaqi, State-of-charge estimation of Li-ion battery in electric vehicles: a deep neural network approach, IEEE Trans. Ind. Appl. 56 (5) (Sep. 2020) 5565–5574, https://doi.org/10.1109/TIA.2020.3004294.
[18] M. Fasahat, M. Manthouri, State of charge estimation of lithium-ion batteries using hybrid autoencoder and long short term memory neural networks, J. Power Sources 469 (Sep. 2020) 228375, https://doi.org/10.1016/j.jpowsour.2020.228375.
[19] D. Darbar, I. Bhattacharya, Application of machine learning in battery: state of charge estimation using feed forward neural network for sodium-ion battery, Electrochem 3 (1) (Jan. 2022) 42–57, https://doi.org/10.3390/electrochem3010003.
[20] E. Almaita, S. Alshkoor, E. Abdelsalam, F. Almomani, State of charge estimation for a group of lithium-ion batteries using long short-term memory neural network, J. Energy Storage 52 (Aug. 2022) 104761, https://doi.org/10.1016/j.est.2022.104761.
[21] S. Wang, F. Wu, P. Takyi-Aninakwa, C. Fernandez, D.-I. Stroe, Q. Huang, Improved singular filtering-Gaussian process regression-long short-term memory model for whole-life-cycle remaining capacity estimation of lithium-ion batteries adaptive to fast aging and multi-current variations, Energy 284 (Dec. 2023) 128677, https://doi.org/10.1016/j.energy.2023.128677.
[22] S. Wang, Y. Fan, S. Jin, P. Takyi-Aninakwa, C. Fernandez, Improved anti-noise adaptive long short-term memory neural network modeling for the robust remaining useful life prediction of lithium-ion batteries, Reliab. Eng. Syst. Saf. 230 (Feb. 2023) 108920, https://doi.org/10.1016/j.ress.2022.108920.
[23] X. Chai, S. Li, F. Liang, A novel battery SOC estimation method based on random search optimized LSTM neural network, Energy 306 (Oct. 2024) 132583, https://doi.org/10.1016/j.energy.2024.132583.
[24] F. Li, W. Zuo, K. Zhou, Q. Li, Y. Huang, State of charge estimation of lithium-ion batteries based on PSO-TCN-attention neural network, J. Energy Storage 84 (Apr. 2024) 110806, https://doi.org/10.1016/j.est.2024.110806.
[25] S. El Fallah, J. Kharbach, Z. Hammouch, A. Rezzouk, M. Ouazzani Jamil, State of charge estimation of an electric vehicle's battery using Deep Neural Networks: simulation and experimental results, J. Energy Storage 62 (Jun. 2023) 106904, https://doi.org/10.1016/j.est.2023.106904.
[26] P. V. C. N. M. S. M. Kollmeyer, LG 18650HG2 Li-ion Battery Data and Example Deep Neural Network xEV SOC Estimator Script, 2020.
[27] ashwin prasad, Decision Trees For Classification (ID3)| Machine Learning Overview of Decision Trees and How to Build One, Medium, https://medium.com/analytics-vidhya/decision-trees-for-classification-id3-machine-learning-6844f026bf1a.
[28] Caglar Aytekin, Neural Networks Are Decision Trees, arvix, 2022.
[29] Eyad Almaita, Saleh Alshkoor, Emad Abdelsalam, Fares Almomani, State of charge estimation for a group of lithium-ion batteries using long short-term memory neural network, J. Energy Storage 52 (2022).
[30] I.H. Sarker, Deep learning: a comprehensive overview on techniques, taxonomy, applications and research directions, SN Comput. Sci. 2 (6) (Nov. 2021) 420, https://doi.org/10.1007/s42979-021-00815-1.
[31] R. Jozefowicz, O. Vinyals, M. Schuster, N. Shazeer, Y. Wu, Exploring the Limits of Language Modeling, arXiv:1602.02410, 2016.
[32] F. Berglund, S. Zaferanlouei, M. Korpås, K. Uhlen, Optimal operation of battery storage for a subscribed capacity-based power tariff prosumer—a Norwegian case study, Energies (Basel) 12 (23) (Nov. 2019) 4450, https://doi.org/10.3390/en12234450.
[33] A. Manoharan, D. Sooriamoorthy, K.M. Begam, V.R. Aparow, Electric vehicle battery pack state of charge estimation using parallel artificial neural networks,

J. Energy Storage 72 (Nov. 2023) 108333, https://doi.org/10.1016/j.est.2023.108333.
[34] J. Meng, G. Luo, M. Ricco, M. Swierczynski, D.-I. Stroe, R. Teodorescu, Overview of lithium-ion battery modeling methods for state-of-charge estimation in electrical vehicles, Appl. Sci. 8 (5) (Apr. 2018) 659, https://doi.org/10.3390/app8050659.
[35] L. Li, C. Wang, S. Yan, W. Zhao, A combination state of charge estimation method for ternary polymer lithium battery considering temperature influence, J. Power Sources 484 (Feb. 2021) 229204, https://doi.org/10.1016/j.jpowsour.2020.229204.
[36] E. Chemali, P.J. Kollmeyer, M. Preindl, A. Emadi, State-of-charge estimation of Li-ion batteries using deep neural networks: a machine learning approach, J. Power Sources 400 (Oct. 2018) 242–255, https://doi.org/10.1016/j.jpowsour.2018.06.104.
[37] X. Fan, W. Zhang, C. Zhang, A. Chen, F. An, SOC estimation of Li-ion battery using a convolutional neural network with U-Net architecture, Energy 256 (Oct. 2022) 124612, https://doi.org/10.1016/j.energy.2022.124612.
[38] Z. Chen, H. Zhao, X. Shu, Y. Zhang, J. Shen, Y. Liu, Synthetic state of charge estimation for lithium-ion batteries based on long short-term memory network modeling and adaptive H-infinity filter, Energy 228 (Aug. 2021) 120630, https://doi.org/10.1016/j.energy.2021.120630.
[39] J. Chen, X. Feng, L. Jiang, Q. Zhu, State of charge estimation of lithium-ion battery using denoising autoencoder and gated recurrent unit recurrent neural network, Energy 227 (Jul. 2021) 120451, https://doi.org/10.1016/j.energy.2021.120451.